10-W-level monolithic dysprosium-doped fiber laser at 3.24 µm

VINCENT FORTIN, FRÉDÉRIC JOBIN, MAXENCE LAROSE, MARTIN BERNIER AND RÉAL VALLÉE

Centre d'optique, photonique et laser (COPL), Université Laval, Québec City, Québec G1V 0A6, Canada

Accepted for publication in *Optics Letters* - 15 December 2018

We report, to the best of our knowledge, the first entirely monolithic dysprosium (Dy)-doped fluoride fiber laser operating in the mid-IR region. The system delivers 10.1 W at 3.24 µm in continuous operation, a record for fiber oscillators in this range of wavelengths. The Dy^{3+} fiber is pumped in-band using an erbium-doped fiber laser at 2.83 µm made in-house and connected through a fusion splice. Two fiber Bragg gratings directly written in the Dy-doped fiber form the 3.24 µm laser cavity to provide a spectrally controlled laser output. This substantial increase of output power in the 3.0 3.3 µm spectral range–could open new possibilities for applications in spec-troscopy and advanced manufacturing.

There is considerable interest in developing high-power mid-IR coherent sources to enable novel applications across a broad range of disciplines. Sources operating in the 3–4 µm spectral range currently find applications in spectroscopy as they can directly probe the fundamental stretch resonances of molecular bonds such as C–H and N–H. This feature makes them a key component for sensing a variety of combustion gases [1], including hydrocarbons [2], as well as various types of explosive materials (e.g., TNT, RDX, PETN, etc.) [3]. The overlap with these strong molecular resonances can also be highly valuable in the advanced manufacturing sector, for instance, to efficiently process polymer materials [4,5].

The direct generation of coherent emission between 3 and 4 µm is, however, an ongoing challenge. Up until now, interband cascade lasers (ICLs) [2] and sources based on nonlinear downconversion processes (e.g., optical parametric oscillators)[6] have been the main technologies addressing applications in this spectral range. However, while the former is currently limited to a few hundred milliwatts at room temperature [7], the latter generally has to rely on complex and cumbersome architectures. Fiber lasers present an attractive alternative as they can produce high power levels, while maintaining a very small footprint. In the last decade, the wavelength coverage of fiber-based sources has been extended to the mid-IR region through the use of fluoride glass (FG) rare-earth-doped fibers. Most efforts to date have focused on scaling up the output power within the 2.8–3.0 µm spectral band, based on either holmium (Ho)-doped [8,9] or erbium (Er)-doped fluoride fibers [10,11]. Most recently, dual-wavelength pumped Erdoped fiber lasers operating in the vicinity of 3.4–3.5 µm have also reached multiwatt level output powers [12]. However, the spectral range between 3.0 and 3.4 µm still remains undeserved, as discussed in Ref. [13]. Dysprosium (Dy)-doped fiber lasers can bridge this spectral gap completely as they possess a broad emission cross section, from 2.6 to 3.4 µm[14]. However, due to the lack of pumping sources around 1.7 µm and the relatively poor efficiency of the 1.1 and 1.3 µm pump schemes resulting from the high quantum defect and strong excited-state absorption processes [15], Dy-doped fiber lasers have not been studied as much as Ho- and Er-doped laser media. Under 1.1 µm pumping, a Dy-doped ZBLAN cavity producing more than 500 mW at 2.98 µm with an efficiency of 18% was recently demonstrated [16]. In another demonstra-tion, a cavity pumped around 1.7 µm exhibited a broad tuning range of ~600 nm (2.81 to 3.38 µm), but with a maximum output power limited to 170 mW [14].

With recent advances in erbium-doped fluoride fiber lasers reaching output powers exceeding 40 W [11], Dy-doped fiber lasers now have access to high power in-band pump sources in the 2.8–3.0 µm region. Since an in-band pumping scheme significantly reduces the pump–signal quantum defect, very high efficiencies can theoretically be achieved (above 80%) with minimal heat generation. Based on such an approach, watt-level emission at 3.15 µm from a Dy:FG fiber laser was recently achieved by Woodward *et al*. [13]. For further power scaling, however, an all-fiber cavity architecture, including a pair of fiber Bragg gratings (FBGs) and a single-mode splice to launch the pump beam in the active fiber, is required.

In this Letter, we report the first monolithic Dy:FG fiber laser, achieved by writing intracore FBGs directly in the gain fiber. The all-fiber system produces 10.1 W of continuous wave (CW) output power at 3.24 µm, a tenfold increase compared to previous reports. Such a laser wavelength is of considerable interest for atmospheric methane detection [17].

The 3.24 μm fiber laser schematic is shown in Fig. 1(a). The laser cavity is made of a 5.5 m Dy-doped zirconium fluoride glass fiber from *Le Verre Fluoré*, having a core diameter of 12.5 μm, a numerical aperture of 0.16, and a Dy doping concentration of 2000 ppm. The core geometry provides single-mode propagation for wavelengths beyond 2.6 μm. The Dy: FG fiber exhibits propagation losses of <20 dB⁄km at 2 μm (as specified by the manufacturer), which are expected to be slightly higher around 3.24 μm. It also has a cladding diameter of 125 μm and is coated with high-index acrylate (i.e., it is single-cladded).

Both FBGs forming the laser cavity at 3.24 μm are written directly in the doped fiber with a femtosecond laser inscription technique involving a phase mask [18]. The inscription of the FBGs was performed through the fiber's polymer coating to maximize their mechanical strength [19], which greatly simplifies fiber handling during the laser assembly process. The transmission spectra of both FBGs are shown in Fig. 2. The input highly reflective (HR)-FBG has a peak reflectivity above 78% and a bandwidth of <0.26 nm (at FWHM). It exhibits transmission losses of ~8% for the 2.83 μm pump and negligible losses at the laser wavelength, as measured by cutback following the laser experiment. To maximize the HR-FBG reflectivity while maintaining low core propagation losses (required for efficient core pumping), the uniform FBG length was increased to 20 mm, and great care was taken to ensure that the photo-induced refractive index change was strictly of type-I (i.e., damage free) to limit photoinduced losses [20]. Since such a long FBG length leads to a narrow reflectivity bandwidth, the peak reflectivity is, therefore, not fully resolved with our 0.1 nm resolution optical spectrum analyzer (OSA, Yokogawa AQ6376). A numerical modeling of the FBG spectral response performed with *OptiGrating* software (Optiwave Systems Inc.) suggests that the peak reflectivity of the HR-FBG is slightly underestimated and should be of the order of 85–90% to fit the measured FBG's transmission spectral response. The output lowly reflective (LR)-FBG was written under similar exposure conditions, but with a chirped phase mask (chirp rate of 1.1 nm/cm) to obtain a low reflectivity of ~20% over a broader bandwidth of ~4nm. The use of a chirped phase mask to write a LR-FBG intrinsically leads to spectral oscillations, as can be seen in Fig. 2. An appropriate apodization profile along the grating could be applied during the writing process to limit these oscillations, which can potentially affect laser stability. The combination of a narrow HR-FBG and a broad LR-FBG ensures a good spectral overlap regardless of the pumping level. Both FBGs were thermally annealed at 75 °C (10 min. for the HR-FBG, 5 min. for the LR-FBG) following the inscription to stabilize their reflectivity.

The pump source consists of an in-house-made all-fiber Er: FG fiber laser delivering a maximum output power of 25 W at 2.83 μm. Its single-mode active fiber has a core size of 15 μm with a NA of 0.12 and an erbium concentration of 70,000 ppm. It supports multimode pumping through its cladding, which has a truncated circular shape measuring 240 × 260 μm. The 6.5 m Er:FG fiber was pumped with a commercial multimode laser diode module at 980 nm, providing up to 115 W of continuous power. The silica fiber delivering the 980 nm pump was directly spliced (S1) to the Er:FG cavity using a splicing procedure similar to [21]. At the output of the erbium-doped fiber laser, a single-mode fusion splice was made with a 1 m undoped fluoride fiber (S2) having a similar core geometry (14 μm diameter, 0.12 NA) and a 250 μm circular cladding. The other end of this undoped fiber was then spliced to the Dy:FG active fiber [S3, also shown in Fig. 1(b)]. Since these two fibers present a slight mode mismatch, the maximum theoretical transmission through the splice is about 93%. In practice, however, the splicing process was very challenging due to the large difference in cladding sizes (i.e., 250 μm versus 125 μm), and a maximum transmission of ~ 87% was actually achieved, as measured by cutback. A cladding mode stripper (CMS) made of gradually increasing refractive index acrylate was applied near splice point S3 to suppress any power propagating in the cladding, either at 980 nm (residual pump) or at 2.83 μm (signal lost through splice S3). All the splices were made with a filament-based splicer (Thorlabs GPX-3400) equipped with an iridium filament.

Proper thermal management is required to protect the laser system from thermal damage at high power levels. The Er:FG cavity was cooled on an aluminum mandrel with V-grooves, whereas the Dy:FG cavity was fixed on an aluminum plate. Since the fiber segment comprising the S3 splice point and the 3.24 μm HR-FBG is subjected to a particularly high thermal load given its residual losses, it was fixed in a V-groove and covered with a copper tape. The section of V-groove holding the HR-FBG was also filled with thermal paste to further reduce the temperature and mitigate spectral instabilities of the laser signal. Since damage to the Dy:FG fiber tip was observed at high power levels, it was necessary to splice a protective end-cap on the output end, as described in Ref. [11]. This degradation is believed to arise from the same OH diffusion process observed in Er-doped fiber lasers near 3 μm[22], even though the output wavelength (3.24 μm) is slightly detuned from the OH absorption peak.

Figure 3 shows the output power at 3.24 μm with respect to the launched pump power at 2.83 μm, measured with a thermopile detector (Gentec UP19K-50F-W5-D0). The laser threshold and slope efficiency are estimated to 1.1 W and 58%, respectively. A maximum output power of 10.1 W was obtained at the maximum available launched pump power (19 W), with no observable saturation of the laser curve. Using an appropriate filter, we also verified that no 2.83 μm residual pump power remained at the laser output.

The laser output spectrum measured with a mid-IR optical spectrum analyzer is shown in Fig. 4. The center wavelength of the spectrum is mainly governed by the narrow HR-FBG. Initially, when the laser is barely above threshold, the spectrum is centered at 3239.13 nm. As the pump power is increased to the maximum level, the wavelength slightly downshifts to 3239.04 nm. This negative spectral drift is primarily caused by a thermal shift of the HR-FBG, which stems from the negative thermo-optic coefficient of fluoride glasses [23]. At all power levels, the output spectrum FWHM is measured to be smaller than 70 pm, a measurement limited by the resolution of the OSA.

The output power stability was also recorded over a 1 h time period, at two different power levels (i.e., around 9.3 W and 4.5 W), as shown in Fig. 5. RMS fluctuations of the order of 0.4% were observed at 9.3 W, while they were somewhat higher (1.1%) at 4.5 W. The reduced stability of the 4.5 W power curve was actually correlated to slight instabilities of the output central wavelength. More specifically, the small jumps in powers observed at 8 and 30 min in Fig. 5(b) correspond to a discrete shift ($\Delta\lambda$ ~ 0.1a€ 0.2nm) of the output spectrum. This is believed to be a consequence of the spectrally oscillating reflectivity structure of the LR-FBG (see Fig. 2), which can allow lasing on several nearby wavelengths. In order to improve the stability of the laser cavity, a LR-FBG with a greater spectral uniformity should be considered. The HR-FBG also contributes to this problem, as it can shift (see Fig. 4) and, in some conditions, get distorted as it is heated by the pump. Therefore, an improved stability is also expected by lowering the pump losses associated to the HR-FBG. Note, however, that it is considerably challenging to entirely suppress the losses at the pump wavelength in a core-pumped laser configuration.

A number of improvements could be made to optimize the laser system. It can be seen that the slope efficiency obtained for the Dy:FG cavity (~58%) is quite far from the maximum achievable Stokes efficiency (87%). Possible improvements include the optimization of the HR-FBG to

increase its reflectivity while minimizing its losses, as well as using a shorter Dy active fiber to limit the reabsorption of the signal at 3.24 μm. Preliminary simulations based on spectroscopic data found in Ref. [15] show that the efficiency could be increased to about 69% by simply reducing the fiber length to 2.2 m (while maintaining all other cavity parameters). Furthermore, by increasing the HR-FBG's reflectivity from 85% to ~99%, a laser slope efficiency of the order of 75% could be reached with a 2 m cavity and a 20% LR-FBG. These simulation results were computed with a propagation loss coefficient of ~50 dB⁄km at 3.24 μm, i.e., the value that gave the best fit of the experimental results displayed in Fig. 3. To reach higher output powers, however, other issues still need to be addressed. The single-mode splice point between the Er:FG fiber laser and the Dy:FG cavity (S3 in Fig. 1) is perhaps the main hurdle to power scaling since its relatively high loss can lead to the fiber failure at high powers. The design of a new Dy-doped fiber having a core and cladding size matching the output of the Er-doped laser (i.e., 15/250 μm) would help to reduce the losses and improve the reproducibility of the splice. In fact, splice losses below 5% are achievable with similar single-mode fluoride fibers, as shown in Ref. [24].

Since the record output power from an Er-doped oscillator now exceeds 40 W [11], we believe Dy-doped fiber cavities delivering output powers exceeding 30 W are within reach. It should be noted that the laser architecture described here is also not strictly restricted to CW operation; it could be easily adapted to operate in the gain-switching regime. Indeed, the 980 nm pumping diodes could be connected to a fast modulator in order to produce sub-μs pulses at 2.8 μm in the Er:FG laser cavity, as recently demonstrated in Ref. [25]. Such high-energy pump pulses would likely induce gain switching of the $^6H_{13/2} \rightarrow {}^6H_{15/2}$ transition in the Dy:FG fiber to generate output pulses in the 3.0–3.3 μm spectral range.

In summary, we have demonstrated a Dy-doped fluoride fiber laser delivering more than 10 W at 3.24 μm in CW operation, a tenfold increase from the previous state of the art. It presents a slope efficiency of about 58% with respect to the 2.83 μm pump, which consists of an Er-doped fluoride fiber laser. The laser source is compact and inherently robust as it is entirely monolithic, without any free-space alignment sections. Further work will focus on the optimization of the laser cavity as well as a redesign of the Dy-doped fiber to match the geometry of the pump (Er-doped) fiber. Applications in material processing and remote sensing in the 3.0–3.3 μm spectral range are likely to benefit from this high-power demonstration.

Funding

Natural Sciences and Engineering Research Council of Canada (NSERC) (IRCPJ469414-13); Canada Foundation for Innovation (CFI) (5180); Fonds de Recherche du Québec-Nature et Technologies (FRQNT) (144616).

Acknowledgment

The authors would like to thank Marc D'Auteuil for technical assistance, as well as Frédéric Maes, Yiğit Ozan Aydin, and Pascal Paradis for helpful discussions.

References

[1] C. S. Goldenstein, R. M. Spearrin, J. B. Jeffries, and R. K. Hanson, Prog. Energy Combust. Sci. 60, 132 (2017).

[2] S. Wang, T. Parise, S. E. Johnson, D. F. Davidson, and R. K. Hanson, Combust. Flame 186, 129 (2017).

[3] M. Kumar, M. N. Islam, F. L. Terry, M. J. Freeman, A. Chan, M. Neelakandan, and T. Manzur, Appl. Opt. 51, 2794 (2012).

[4] J. L. Koenig, Spectroscopy of Polymers (Elsevier, 1999).

[5] C. Frayssinous, V. Fortin, J.-P. Bérubé, A. Fraser, and R. Vallée, J. Mater. Process. Technol. 252, 813 (2018).

[6] S. Veerabuthiran, A. K. Razdan, M. K. Jindal, R. K. Sharma, and V. Sagar, Opt. Laser Technol. 73, 1 (2015).

[7] D. Jung, S. Bank, M. L. Lee, and D. Wasserman, J. Opt. 19, 123001 (2017).

[8] S. D. Jackson, Opt. Lett. 34, 2327 (2009).

[9] S. Crawford, D. D. Hudson, and S. D. Jackson, IEEE Photon. J. 7, 1 (2015).

[10] V. Fortin, M. Bernier, S. T. Bah, and R. Vallée, Opt. Lett. 40, 2882 (2015).

[11] Y. O. Aydin, V. Fortin, R. Vallée, and M. Bernier, Opt. Lett. 43, 4542 (2018).

[12] F. Maes, V. Fortin, M. Bernier, and R. Vallée, Opt. Lett. 42, 2054 (2017).

[13] R. Woodward, M. R. Majewski, G. Bharathan, D. Hudson, A. Fuerbach, and S. D. Jackson, Opt. Lett. 43, 1471 (2018).

[14] M. R. Majewski, S. D. Jackson, and R. Woodward, Opt. Lett. 43, 971 (2018).

[15] L. Gomes, A. F. H. Librantz, and S. D. Jackson, J. Appl. Phys. 107, 053103 (2010).

[16] L. Sójka, L. Pajewski, M. Popenda, E. Beres-Pawlik, S. Lamrini, K. Markowski, T. Osuch, T. M. Benson, A. B. Seddon, and S. Sujecki, IEEE Photon. Technol. Lett. 30, 1083 (2018).

[17] M. Ghysels, L. Gomez, J. Cousin, N. Amarouche, H. Jost, and G. Durry, Appl. Phys. B 104, 989 (2011).

[18] M. Bernier, D. Faucher, R. Vallée, A. Saliminia, G. Androz, Y. Sheng, and S. L. Chin, Opt. Lett. 32, 454 (2007).

[19] M. Bernier, F. Trépanier, J. Carrier, and R. Vallée, Opt. Lett. 39, 3646 (2014).

[20] K. Itoh, W. Watanabe, S. Nolte, and C. B. Schaffer, MRS Bull. 31(8), 620 (2011).

[21] R. Carbonnier and W. Zheng, Proc. SPIE 10513, 105131G (2018).

[22] N. Caron, M. Bernier, D. Faucher, and R. Vallée, Opt. Express 20, 22188 (2012).

[23] J. M. Jewell and I. D. Aggarwal, J. Non-Cryst. Solids 142, 260 (1992).

[24] V. Fortin, M. Bernier, N. Caron, D. Faucher, M. El Amraoui, Y. Messaddeq, and R. Vallée, Opt. Eng. 52, 054202 (2013).

[25] P. Paradis, V. Fortin, Y. O. Aydin, R. Vallée, and M. Bernier, Opt. Lett. 43, 3196 (2018).

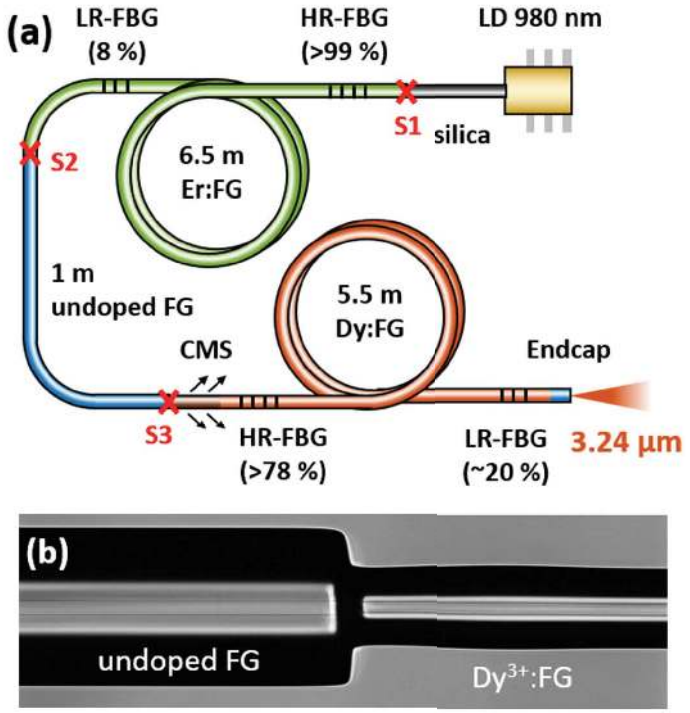

Fig. 1. (a) Experimental setup of the 10-W-level Dy-doped fluoride fiber laser at 3.24 µm. CMS, cladding mode stripper; LD, laser diode; S1, multimode splice point; S2–S3, single-mode splice points. (b) Microscope image of the fusion splice (S3) between the undoped FG fiber and the Dy:FG fiber.

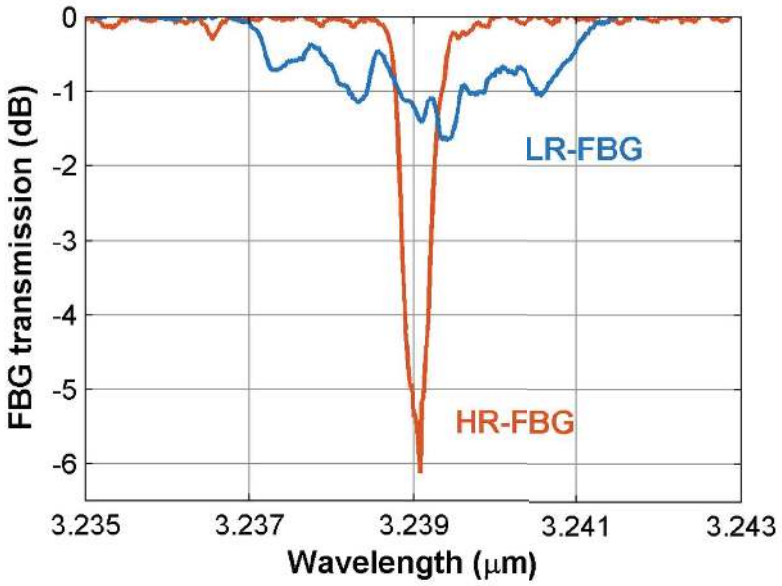

Fig. 2. Transmission spectrum of HR- and of LR-FBGs bounding the 3.24 μm laser cavity.

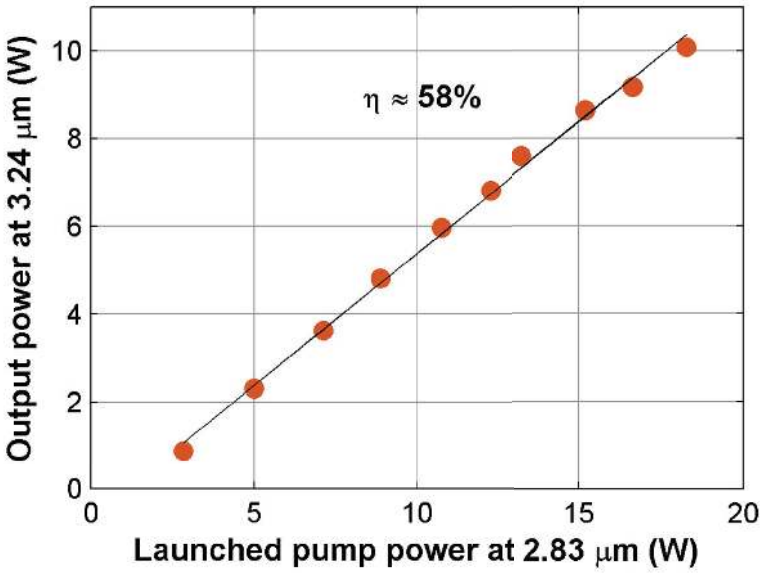

Fig. 3. Laser output power at 3.24 μm as a function of the launched pump power at 2.83 μm. The average slope efficiency is 58%.

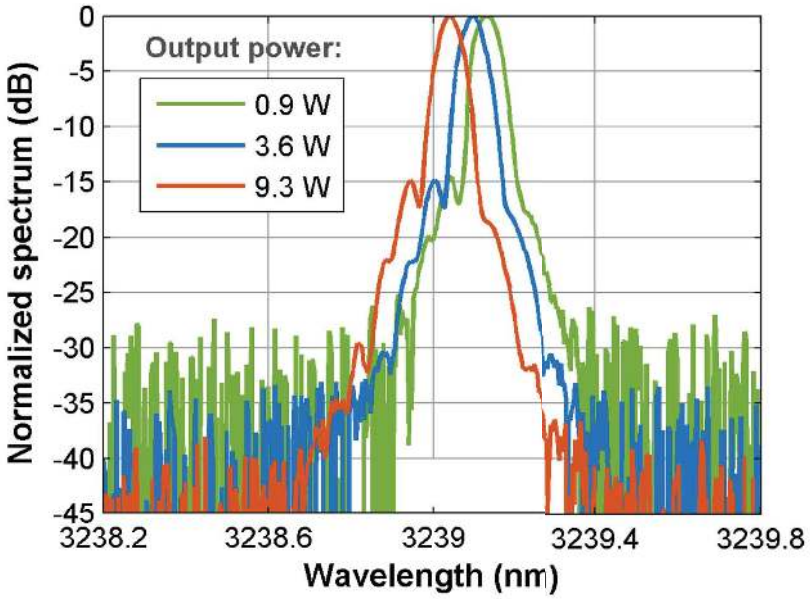

Fig. 4. Output spectrum of the Dy:FG fiber laser at output powers of 0.9, 3.6, and 9.3 W.

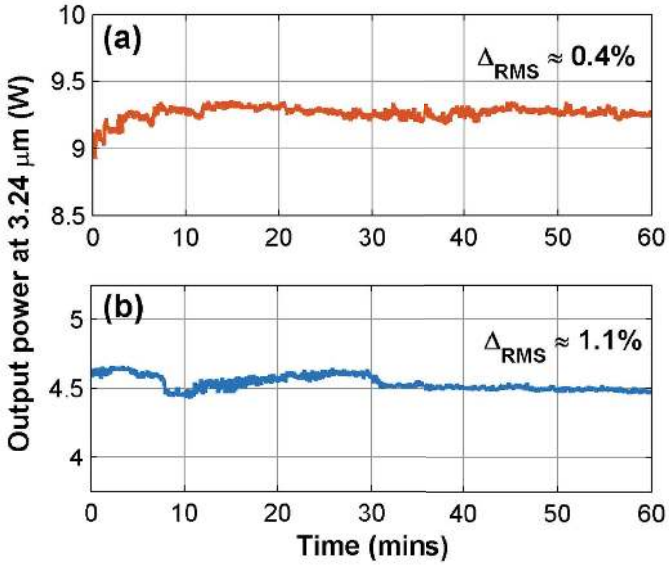

Fig. 5. Output power stability around (a) 9.3 W and (b) 4.5 W at 3.24 μm, showing respective RMS variations of 0.4% and 1.1%.